First-principles theoretical description of electronic transport including electron-electron correlation

A. Ferretti,* A. Calzolari, R. Di Felice, and F. Manghi
National Research Center on nanoStructures and bioSystems at Surfaces (S^3), INFM-CNR and Dipartimento di Fisica, Università di Modena e Reggio Emilia, 41100 Modena, Italy
(Received 28 December 2004; revised manuscript received 7 July 2005; published 20 September 2005)

We report about the inclusion of many-body electron interactions in the simulation of transport properties. We derive a general Landauer-like expression for the current, valid also in the case of conductors in which the charge carriers undergo generic scattering processes. An important focus is put on the derivation of the theoretical framework, both for the general formalism and for the actual implementation of the method, including the treatment of electronic correlation. We then show an example of application and compare the results on the electronic and conduction properties obtained with our new scheme to those given by alternative computational frameworks.

DOI: 10.1103/PhysRevB.72.125114 PACS number(s): 73.63.−b, 71.28.+d, 72.10.−d

I. INTRODUCTION

In order to continue to scale down the size of electronic devices, modern science and technology are currently engaged in replacing the usual top-down lithographic approach to device fabrication with an alternative scheme[1–11] that would start from *ad hoc* nanosized building blocks such as, e.g., carbon nanotubes or molecules. In this scenario a large effort is being devoted to develop theoretical and computational tools able to describe transport properties of systems obtained connecting two (or more) electrodes with a bridging nanoscale unit. A detailed theory of transport in *mesoscopic* systems has been known for a long time, but the matching of those ideas with the new problems arising in *nanoscopic* objects is not obvious. One needs to describe at the same time an open and nonperiodic system, as well as details of the bridging conductor at the atomic level (this is fundamental in the case of molecular conductors, for example).

Furthermore, the use of standard electronic structure approaches based on density functional theory (DFT) for calculating transport properties is not straightforward and suffers from additional problems in the description of nanodevices. Even if not rigorously exact for transport theory, DFT is quite well established and it is usually easy to recognize reliable from out-of-scope results. We can roughly separate the problems for DFT in the new field of nanoscience in two blocks. The first comprises questions on the applicability of DFT to the transport properties in the out-of-equilibrium situation: Few such schemes already exist,[12–14] but several open questions about the internal consistency of the method arose from some claimed (but reproducible) quantitative failures.[15] The second block of problems concerns the emergence—or even dominance—of other effects, not well described in standard DFT approaches, in the extremely confined systems representative of nanoscale conductors. This is typically the case of electron-phonon coupling or electron-electron (*e-e*) interaction. Recent experiments have in fact demonstrated that some well-known mesoscopic effects,[16] such as Coulomb blockade,[17–20] Kondo effect[19,21,22] or Luttinger-liquid behaviors,[2,23,24] occur also in the case of nanoscale conductors. In view of these findings a suitable description of *e-e* interaction effects in the treatment of transport is highly desirable: New formulations including these effects[25–29] are appearing, but a standard approach does not yet exist.

In the present work we tackle the problem of including *e-e* interactions in transport simulations within an *ab initio* framework. Along this line, we first derive a general *Landauer-like* expression for the current and thus define an effective transmittance across the conductor accounting also for interactions among charge carriers and scatterers. We propose a specific implementation and apply our scheme to the case of a finite, short platinum atomic chain between leads, modeling a prototypical break-junction. We focus on the short-range *e-e* correlation regime, and model the junction by turning on the interaction only in the confined conductor. The calculation requires the use of maximally localized Wannier functions[30,31] for the basis set, and a matrix Green's functions (GF's) framework[32] in the WANT code.[33] Our results demonstrate that both the conductance and the transmittance across the conductor are renormalized by the interactions. We also show that a large part of the effect can be ascribed to the incoherent component of charge motion, arising from a genuine many-body treatment of the *e-e* interaction. We enforce this interpretation by means of a comparison with the well established LDA+U scheme.[34–36]

The paper is organized as follows. In Sec. II we first give (Sec. II A) a critical survey of the general expression for the current obtained by Meir and Wingreen,[37] then we explicitly derive (Sec. II B) a Landauer-like formula valid also in the interacting regime, and finally describe (Sec. II C) the relation of this formalism with a scattering picture. In Sec. III we give the details of the actual first principles implementation of the method, including (Sec. III A) the description of the mean-field transport approach using maximally localized Wannier functions and (Sec. III B) the approach to treat electronic correlation. In Sec. IV we describe the system that was selected for a prototype application. We analyze the results that were obtained with the new computational method and compare them to those given by the LDA+U framework. In

the Appendix we give some more details on the out-of-equilibrium framework used throughout the paper.

II. FORMALISM

A. The current through a lead-conductor-lead junction

Let us consider a system composed of three main regions, two leads [that we label left (L) and right (R)] and a central conductor (C) connecting them. By using a localized basis set, it is possible to take advantage of this geometry and relate each basis element to a precise region, thus writing the Hamiltonian and other operators of interest in block-matrix form, i.e., $H_{XY}=\{H_{ij}\}, i\in X, j\in Y$ where $X,Y=L,C,R$. The L-C-R junction may be described by the following Hamiltonian:

$$H=\sum_{ll'\in L \text{ or } R} H_{ll'}c_l^\dagger c_{l'}+H_C+\sum_{\substack{l\in L \text{ or } R\\ i\in C}}(H_{li}c_l^\dagger d_i+\text{h.c.}). \tag{1}$$

Here, c_l and d_i ($c_l^\dagger$ and $d_i^\dagger$) are annihilation (creation) operators in the leads and conductor, respectively, while H_C represents a general Hamiltonian including two-body interactions acting in the C region (written by means of $\{d_i\}$ and $\{d_i^\dagger\}$). In this picture the description of the leads is cast at the single particle level, while only the coupling between the leads and the conductor region makes the problem to be fully interacting. Physically, this approximation is justified by the large screening of the Coulomb interaction, which takes place in usually adopted metallic leads. The assumption breaks down in the presence of metals with a high degree of charge localization and consequent less effective screening, such as some d or f metals and their oxides.

In a seminal work,[37] Meir and Wingreen define the current flowing through a lead-conductor-lead junction as the time derivative of the number operator of one lead, namely $N_X=\Sigma_{l\in X}c_l^\dagger c_l$ where $X=L,R$. The current entering the L region can then be written as

$$I_L=-e\langle\dot{N}_L\rangle=-\frac{ie}{\hbar}\langle[H,N_L]\rangle, \tag{2}$$

where the averages given by $\langle\cdot\rangle$ are defined on a suitable nonequilibrium statistics. Doing the algebraic calculations for the commutators, the current turns out to be expressed as

$$I_L=\frac{e}{\hbar}\int\frac{d\omega}{2\pi}\text{Tr}[G_{CL}^<(\omega)H_{LC}-H_{CL}G_{LC}^<(\omega)], \tag{3}$$

where summations have been hidden in the block-matrix multiplication notation and the trace should be taken on the conductor basis elements, including spin degrees of freedom. $G_{il}^<(t_1-t_2)=i\langle c_l^\dagger(t_1)d_i(t_2)\rangle$ is the lesser Green's function and $G_{il}^<(\omega)$ is its Fourier transform wrt t_1-t_2.[38]

It is interesting to note that, should the interaction term in the Hamiltonian of Eq. (1) be spread over the entire L-C-R junction, instead of being localized in H_C only, a further term in the current would appear, generated by a two-particle GF:

$$\Delta I_L=\frac{e}{\hbar}\,\text{Im}\sum_{\substack{ijk\in LCR\\ l\in L}}\langle c_i^\dagger c_j^\dagger c_k c_l\rangle(V_{ijkl}-V_{ijlk}), \tag{4}$$

where V is the two-body spread interaction. It is possible to translate this expression in terms of some interaction energy expectation values. This indicates that the approximation of the Hamiltonian as in Eq. (1) means treating at the mean-field level the energy fluctuations of the Coulomb interaction that involve the leads. In turn, it implies that such fluctuations are neglected as driving forces for current flow. As mentioned before, this approximation is at the basis of our treatment and is well justified for the class of physical systems under investigation (e.g., organic nanodevices). It yields an important reduction of the complexity of the whole theory, by avoiding the inclusion of two-particle GF's.

From Eq. (3) and using the Keldysh nonequilibrium GF techniques[38,39] (for the specific details see Appendix A of Ref. 40) it is possible to write the final expression for the current given by Meir and Wingreen:

$$I=\frac{e}{2h}\int d\omega\text{Tr}[(f_L\Gamma_L-f_R\Gamma_R)A_C+i(\Gamma_L-\Gamma_R)G_C^<]. \tag{5}$$

Here $A_C=i(G_C^r-G_C^a)$ is the spectral function and $G_C^{r,a,<,>}$ are the (retarded, advanced, lesser, greater) Green's functions in the conductor. As in Eq. (3), the trace should be taken on the conductor basis states (including spin). The terms $\Gamma_{L,R}$ represent the coupling matrices with the L and R leads and are defined as

$$\Gamma_X=i(\Sigma_X^r-\Sigma_X^a),$$

$$\Sigma_X^{r,a}=H_{CX}g_X^{r,a}H_{XC},\quad \text{where } X=L,R. \tag{6}$$

In the latter expression, $g_X^{r,a}$ are the retarded and advanced GF's of the X lead, which is considered to be in equilibrium, with Fermi occupation function $f_X(\omega)$. Note also that $\Sigma_{L,R}^<=if_{L,R}\Gamma_{L,R}$ and $\Sigma_{L,R}^>=-i(1-f_{L,R})\Gamma_{L,R}$.

Both terms in Eq. (5) reflect the composition of the current as a combination of three ingredients: (*i*) the coupling between the conductor and the leads, accounted for by the Γ's; (*ii*) the energy levels in the conductor, given by the spectral function $A_C(\omega)$; and (*iii*) the occupations of energy levels, given by $f_{L,R}(\omega)$ for the leads and by $G_C^<(\omega)$ for the conductor. Indeed, while in the equilibrium case the fluctuation-dissipation theorem[38] gives $G_C^<(\omega)=if_C(\omega)A_C(\omega)$, which is by definition a relation between the lesser and the retarded GF's, in the general out-of-equilibrium case no similar relations exist and the "occupations" in the conductor should be determined by the so-called Keldysh equation for $G^<$, to be solved together with the Dyson equation for G^r,[38] namely,

$$G_C^{<,>}(\omega)=G_C^r(\omega)\Sigma_C^{<,>}(\omega)G_C^a(\omega), \tag{7}$$

$$G_C^{r,a}(\omega)=G_{0,C}^{r,a}(\omega)+G_{0,C}^{r,a}(\omega)\Sigma_C^{r,a}(\omega)G_C^{r,a}(\omega). \tag{8}$$

$G_{0,C}^{r,a}$ are the reference noninteracting (retarded, advanced) GF's for the C region and $\Sigma_C^{<,>}(\omega),\Sigma_C^{r,a}(\omega)$ are the self-

energies for the interacting system that should be determined by suitable approximations.

B. A generalized *Landauer-like* formula

If the interaction term in H_C of Eq. (1) is neglected, one is left with a mean-field description of the system and further analysis can be carried out. The mean-field quantities are identified here by the subscript 0. An expression for $G_{0C}^{<,>}$ is available for the (mean-field) out-of-equilibrium regime (details in the Appendix)

$$G_{0C}^{<,>} = G_{0C}^{r}(\Sigma_{L}^{<,>} + \Sigma_{R}^{<,>})G_{0C}^{a}, \tag{9}$$

which is equivalent [cf. Eq. (7)] to the definition of the noninteracting lesser and greater self-energies as $\Sigma_{0,C}^{<,>} = \Sigma_{L}^{<,>} + \Sigma_{R}^{<,>}$. Subtracting the lesser and greater terms in Eq. (9) and using the definition $G^r - G^a = G^> - G^<$, valid for any Green's function, one easily derives

$$G_{0C}^{r} - G_{0C}^{a} = -iG_{0C}^{r}(\Gamma_L + \Gamma_R)G_{0C}^{a}. \tag{10}$$

Inserting Eqs. (9) and (10) into Eq. (5) and taking into account that $\Gamma_L G_{0C}^{r}\Gamma_R G_{0C}^{a} = \Gamma_R G_{0C}^{r}\Gamma_L G_{0C}^{a}$ by virtue of the particle number conservation in the whole system, one arrives to the so-called Landauer formula,[41] as originally expressed by Fisher and Lee:[42]

$$I = \frac{e}{\hbar}\int \frac{d\omega}{2\pi}(f_L - f_R)\mathrm{Tr}(\Gamma_L G_{0C}^{r}\Gamma_R G_{0C}^{a}). \tag{11}$$

This equation connects transport quantities, such as the current or the zero-temperature conductance, to a scattering quantity like the transmittance across the scattering region (the trace term in the previous equation), thus allowing for a deeper insight into the mechanism of ballistic transport itself. All this formalism and its interpretation break down when any many-body coupling among charge carriers is switched on in the conductor.

In order to correctly introduce correlation effects in transport calculations we adopted[29] an *ansatz* previously proposed in the literature,[43,44] to connect retarded and lesser GF's in the general interacting out-of-equilibrium case. According to this *ansatz*, the matrices $\Sigma_C^{<,>}$ that appear in Eq. (7) are defined as

$$\Sigma_C^{<}(\omega) = \Sigma_{0C}^{<}(\omega)\Lambda(\omega),$$

$$\Sigma_C^{>}(\omega) = \Sigma_{0C}^{>}(\omega)\Lambda(\omega). \tag{12}$$

$\Lambda(\omega)$ is a suitable dynamical operator to be determined by imposing the well-known identity $\Sigma^> - \Sigma^< = \Sigma^r - \Sigma^a$. The above definitions lead to an explicit expression for $\Lambda(\omega)$ which reads

$$\Lambda(\omega) = [\Sigma_{0C}^{r}(\omega) - \Sigma_{0C}^{a}(\omega)]^{-1}[\Sigma_C^{r}(\omega) - \Sigma_C^{a}(\omega)], \tag{13}$$

where $\Sigma_{0C}^{r,a} = \Sigma_L^{r,a} + \Sigma_R^{r,a} \mp i\delta^+$ as in mean field and $\Sigma_C^{r,a} = \Sigma_L^{r,a} + \Sigma_R^{r,a} \mp i\delta^+ + \Sigma_{corr}^{r,a}$. The $\Sigma_{corr}^{r,a}$ term is a contribution to the self-energy operators due specifically to the presence of an electron-electron interaction in the system (more details are in the Appendix). The *ansatz* is obviously valid in the *nonequilibrium mean-field* case by definition (just setting Λ equal to the identity), but it is also exact in the *equilibrium many-body* case, since in equilibrium conditions the fluctuation-dissipation theorem holds, and the G^r and $G^<$ are no longer independent. An exact relation to connect Σ^r and $\Sigma^<$ should exist in any equilibrium situation, even in the presence of many-body couplings among charge carriers. The *ansatz* of Eq. (12) generalizes the existence of a relation between G^r and $G^<$ to the *nonequilibrium many-body* case, by inspiration from the two exact limits described above, i.e., *nonequilibrium mean-field* and *equilibrium many-body*. It can be viewed as a tool partly playing the role of the fluctuation-dissipation theorem itself. This approximation has already been used to tackle different physical situations such as the Kondo effect and the Anderson model[43–45] (in the time-dependent or spin-polarized limits), as well as the Luttinger-Marginal Fermi liquids.[46]

With a simple algebra Eq. (13) can also be written as

$$\Lambda(\omega) = \mathbb{I} + (\Gamma_L + \Gamma_R + 2\delta^+)^{-1}\Gamma_{corr}, \tag{14}$$

$\Gamma_{corr} = i(\Sigma_{corr}^{r} - \Sigma_{corr}^{a})$ being twice the imaginary part of the retarded correlation SE. The Λ correction reads therefore as the identity (noninteracting limit) plus the ratio between two Γ factors, namely the one representing the *e-e* interaction, and the one representing the conductor-lead coupling. From this expression, we expect that Λ would significantly differ from zero only in the limit of weak coupling with leads, because in the case of strong coupling one would most likely have $|\Gamma_L + \Gamma_R| \gg |\Gamma_{corr}|$, and consequently $\Lambda \simeq \mathbb{I}$. One example of this limit in the interacting case may be the Coulomb blockade regime.

Once an explicit form of $\Sigma_C^{<}(\omega)$ is known in terms of $\Sigma_C^{r,a}(\omega)$, one can write down the two following crucial equations:

$$G_C^{<,>} = G_C^{r}(\Sigma_L^{<,>} + \Sigma_R^{<,>})\Lambda G_C^{a}, \tag{15}$$

$$G_C^{r} - G_C^{a} = -iG_C^{r}(\Gamma_L + \Gamma_R)\Lambda G_C^{a}. \tag{16}$$

These are formally analogous to Eqs. (9) and (10) that allow us to obtain the Landauer formula Eq. (11) from the Meir-Wingreen expression for the current, Eq. (5). Thus, they can be used in the same way to write a general "Landauer-like" expression[29] which is approximately valid also in the general out-of-equilibrium many-body case:

$$I = \frac{e}{\hbar}\int \frac{d\omega}{2\pi}(f_L - f_R)\mathrm{Tr}(\Gamma_L G_C^{r}\Gamma_R \Lambda G_C^{a}). \tag{17}$$

Here, the inclusion of electronic correlation gives a twofold effect, namely the presence of the corrective term Λ and the renormalization of the conductor GF's, which no longer have the subscript 0 as in the noninteracting case of Eq. (11). We note that the same formula was also obtained by Meir and Wingreen[37] in a special case of their formulation and by Zhang and co-workers.[45] While their applications were devoted to empirical model, here we focus on an atomistic *ab initio* implementation of the method.

C. Relation to scattering properties

A direct comparison of Eq. (17) with the Landauer formula (which is equal except for the presence of Λ and the mean-field Green's functions) gives a scattering interpretation also in the many-body case. In fact, the trace in Eq. (11) is identified as the transmittance (across the C region) in the mean-field case. In analogy, the term $\mathrm{Tr}(\Gamma_L G_C^r \Gamma_R \Lambda G_C^a)$ in Eq. (17) plays the same role in the many-body case and can be defined as an *effective transmittance*, $T_{\mathrm{eff}}(\omega)$, for what concerns the role in transport phenomena. This is an important observation, because it implies that the introduction of *e-e* interactions can be interpreted *a posteriori* in terms of the renormalization of a well-defined quantity, characterized by a simple and straightforward interpretation.

From Eq. (17) we are also able to obtain an expression for the conductance at zero temperature, just deriving the current wrt the applied voltage (i.e., the difference between the Fermi levels of the L and R leads) and setting $\omega = E_f$, as in the standard Landauer approach. The result reads

$$G = \frac{e^2}{h} T_{\mathrm{eff}}(E_f) = \frac{e^2}{h} \mathrm{Tr}(\Gamma_L G_C^r \Gamma_R G_C^a)_{\omega = E_f}, \tag{18}$$

which is exactly the same result obtained in the mean-field case, except that GF's are renormalized by the *e-e* interaction. The Λ factor disappears here because it is evaluated at the Fermi level of the whole system (we are in the limit of almost vanishing bias voltage in which the equilibrium is reestablished), where the imaginary part of the correlation self-energy $\Sigma_{corr}^r - \Sigma_{corr}^a$ vanishes by definition, thus leading to $\Lambda(E_f) = \mathbb{I}$ in Eqs. (13) and (14).

Other formulations[15,47,48] based on time-dependent extensions of DFT (or current DFT)[49,50] recognize the validity of a single-particle Landauer formula also in the fully interacting case. This is *not* in contrast with the present work: it is just a different approach to make a complex problem computationally tractable. In TDDFT one defines a fictitious auxiliary noninteracting system whose time-dependent density is equal to the actual one.[49] Therefore, the GF's and lead SE's entering the Landauer formula are calculated for the auxiliary system and hence are not the same quantities we use here. That is why the Landauer formula is recovered exactly in the form of Eq. (11), but with operators computed for the auxiliary system. We note that in this approach some genuine many-body quantities, such as the spectral features or the electronic structure, are not rigorously obtained. On the contrary, our many-body approach contains a much larger amount of information through the interacting GF's. The main drawback is the larger computational complexity. Hybrid approaches have been recently proposed.[51]

In closing this section, we wish to emphasize that one of the main advantages of Eq. (17) over its exact counterpart Eq. (5) is the possibility of identifying an *effective transmittance*. This is useful in order to give a deeper physical insight based on a scattering point of view, such as, e.g., eigenchannel analyses. It is also possible to study the linearized behavior of the current without explicitly facing the out-of-equilibrium problem. The outcome is a useful way to separate the effect of introducing correlation and that of handling the mean-field nonequilibrium situation, which is still open and controversial.[15]

III. IMPLEMENTATION

We numerically implemented the method described above in two steps: first we used the recently released WANT package[33] for the calculation of coherent transport properties based on the DFT electronic structure and on the use of maximally localized Wannier functions (MLWF's) as basis set; then we generalized the above formulation to the case in which an *e-e* interaction is switched on in the conductor. We developed the new computational framework by merging the WANT treatment of the real space GF method with a suitable way of computing the electron-electron SE's. The SE's are dealt with here for the case of short-range correlations by means of a nonperturbative approach based on solving an effective Anderson Hamiltonian.[52] The adopted SE approach is known as the three-body scattering (3BS) method.[53,54]

A. Coherent transport using maximally localized Wannier functions

The treatment of the transport problem, in the present description, needs a localized basis set in order to take advantage of the different physical properties of the various regions (L, C, R) that compose the system. It was recently proposed[55] that such a basis set could be obtained by computing the maximally localized Wannier functions (WF's) through the algorithm given by Marzari and Vanderbilt,[30,31] starting from a plane wave electronic structure calculation. Plane-wave implementations of DFT are very popular and successful in the solid state research community. The combination of WF's and GF's techniques for the transport problem was developed in the WANT package. The use of WF's gives highly desirable features such as the completeness of the basis in a chosen subset of eigenvectors of the system and the orthonormality of the localized basis. Whereas the second issue is useful from a practical point of view, the first one is of fundamental importance to solve—in principles—some typical difficulties in the representability (under- and over-completeness) of wave functions on other localized bases.

The WANT method is based on a DFT computation of the electronic structure of the system. The code is interfaced with the PWscf (Ref. 56) package which adopts plane waves as basis set and pseudopotentials to describe the ions.

Given a periodic system and its Bloch eigenstates $|m\mathbf{k}\rangle$ computed with the PWscf code, the ith WF at site $\mathbf{R}$ can be defined as

$$|i\mathbf{R}\rangle = \frac{1}{N_k} \sum_{\mathbf{k} \in \mathrm{BZ}} e^{-i\mathbf{k}\cdot\mathbf{R}} \sum_m U_{im}(\mathbf{k}) |m\mathbf{k}\rangle, \tag{19}$$

where the sum for $\mathbf{k} \in \mathrm{BZ}$ runs over the N_k uniform $\mathbf{k}$ points in the Brillouin zone and $U(\mathbf{k})$ is a unitary matrix mixing different bands at the same $\mathbf{k}$. This form ensures the orthonormality and the completeness stemming from the properties of the Bloch states. The matrix $U(\mathbf{k})$ represents a further set of degrees of freedom which have been used to maximize

the localization of the resulting WF's. In practice, a spread functional is defined as

$$\Omega[U] = \sum_i (\langle i\mathbf{0}|\mathbf{r}^2|i\mathbf{0}\rangle - \langle i\mathbf{0}|\mathbf{r}|i\mathbf{0}\rangle^2). \quad (20)$$

The larger is Ω for a given a set of $\{U(\mathbf{k})\}$, the more extended in space are the WF's. For our purposes, $\Omega[U]$ must be iteratively minimized with respect to the $\{U(\mathbf{k})\}$ matrix to attain the desired maximal localization. For a full description see Refs. 30 and 31.

In order to solve the transport problem we need to compute the WF's for the L,C,R regions and the mean-field Hamiltonians on such a basis. Three sets of calculations are needed for the L and R leads and the C conductor. DFT calculations are performed by applying periodic boundary conditions to a unit supercell. One needs to include in the conductor supercell a part of each lead that should be large enough to reproduce the behavior of the respective bulk at the edges of the cell. This is required in order to enable a well-defined matching of the three regions, and it is also useful to extract the H_{CL} and H_{CR} Hamiltonian blocks entering the lead SE's calculation from the conductor Hamiltonian. The WANT scheme applied with this care contains all the ingredients for the computation of the mean-field transmittance through the C region according to Fisher and Lee as described in Sec. II C. Further details are in Ref. 55. In the next section we show how this method can be complemented by an accurate description of the SE's to go beyond the mean-field restriction.

B. Introduction of many-body effects

Electron-electron interactions are directly accounted for via the inclusion of a related SE operator. It is important to stress here that the large part of the mean-field machinery for transport calculations (e.g., the evaluation of lead self-energies and related quantities) can be used also in the presence of interactions: this property is desired for the implementation of a Landauer-like formula as Eq. (17). This has clearly important consequences in the actual implementation of the method. Moreover, due to the fact that we aim at computing equilibrium properties such as the effective transmittance, the *e-e* retarded SE is easily connected to the lesser one and thus we need to compute just one of them.

The way the SE is calculated depends on the system under study and therefore on the specific range of correlation. In this work we focus on the case of short-range interactions used to model conductors with highly localized orbitals (typical cases in transition metals). We include some effective on-site Anderson terms and consistently avoid double counting by eliminating the respective mean-field terms. We then compute the self-energy for the conductor region (which must contain part of the leads, as described above) considering a fictitious periodicity (supercell approximation). This is important in order to simulate the nonfiniteness of the open system without treating it explicitly, giving the correct thermodynamic limit and analytical properties of the interacting GF's.[57,58] The conductor Hamiltonian in the presence of Hubbard-like *e-e* interactions reads [see Eq. (1)]

$$H_C = \sum_\sigma \sum_{ij\in C} H_{ij,\sigma} d^\dagger_{i,\sigma} d_{j,\sigma} + \frac{1}{2}\sum_\sigma \sum_{pq} (U_{pq} - J_{pq}) n_{p,\sigma} n_{q,\sigma} + \frac{1}{2}\sum_\sigma \sum_{pq} U_{pq} n_{p,\sigma} n_{q,-\sigma}, \quad (21)$$

where site and spin indexes are explicitly separated, U_{pq} and J_{pq} are the direct and exchange Coulomb integrals, and $n_{p,\sigma}$ is the density operator for orbital p. Indexes p and q run over the orbitals defined on sites where charge carriers are correlated. The U and J matrices do not couple orbitals on different sites. We remark that the ij orbitals on which the first term in the Hamiltonian of Eq. (21) is expressed belong to a generic basis set (and we will assume them to be the computed Wannier functions presented in Sec. III A). Differently, the pq orbitals used in the second and third terms (i.e., the orbitals on sites where U and J are switched on) have a different meaning: they should carry the physical information on correlated electrons. The WF's could not be used in these terms because of their intrinsic nonuniqueness. We thus decide to define the pq orbitals in Eq. (21) as the d- or f-atomic orbitals present in the system. At the end of its evaluation, the correlation self-energy is finally expressed on the WF's basis in order to be inserted in the transport calculation.

The solution of the Hamiltonian in Eq. (21) (e.g., in terms of GF's) is not straightforward in the general case and some further approximations are needed. Here we adopt a scheme[53,54] which is nonperturbative in the U/t parameter; t is a measure of the mean-field hopping term given by $H_{ij,\sigma}$ in Eq. (21). The nonperturbative approach allows us to focus on the regime $U \simeq t$, which is forbidden by alternative schemes designed specifically to solve the two perturbative limits $U/t \to 0$ and $t/U \to 0$. The method is based on a configuration interaction expansion of the states with one particle (an electron or a hole) added to the Fermi sea. This expansion is truncated after a certain number N_{eh} of electron-hole pairs is added to the state with $N \pm 1$ electrons. With the choice to cut the expansion within one added electron-hole pair, the problem can be recast as an effective three-body scattering (3BS) and its solution determines the GF for the original Hamiltonian. Because the generic Hubbard Hamiltonian H is periodic in real space, we move to the basis of Bloch eigenvectors $\{a_{\mathbf{k}m\sigma}\}$ of the mean-field problem, defining the electron $(+)$ and hole $(-)$ GF according to the Lehmann representation:[58]

$$G^+_{\mathbf{k}m\sigma n\sigma'}(\omega) = \langle GS|a_{\mathbf{k}m\sigma}\frac{1}{z-H}a^\dagger_{\mathbf{k}n\sigma'}|GS\rangle, \quad (22)$$

$$G^-_{\mathbf{k}m\sigma n\sigma'}(\omega) = \langle GS|a^\dagger_{\mathbf{k}n\sigma'}\frac{1}{z-H}a_{\mathbf{k}m\sigma}|GS\rangle, \quad (23)$$

where $z=\omega+E_0[N]+i\eta^+$ for electrons and $z=\omega-E_0[N]-i\eta^+$ for holes, $E_0[N]$ being the energy of the many-body ground state (GS) with N electrons (indicated as $|GS\rangle$). In order to calculate the GF, one needs to evaluate the Hamiltonian H in the subspace related to $N+1$ and $N-1$ electron states for G^+ and G^-, respectively. The expansion of the $N-1$ Hamiltonian

up to three bodies added to the mean-field ground state ($|GS_0\rangle$) contains, for each $\mathbf{k}$ and σ, the terms

$$|s^-\rangle = a_{\mathbf{k}m\sigma}|GS_0\rangle,$$

$$|t^-\rangle = a^\dagger_{\mathbf{q}_1 m_1 \sigma_1} a_{\mathbf{q}_2 m_2 \sigma_2} a_{\mathbf{q}_3 m_3 \sigma_3}|GS_0\rangle, \tag{24}$$

where

$$\mathbf{q}_1 - \mathbf{q}_2 - \mathbf{q}_3 = \mathbf{k}, \quad \sigma_1 - \sigma_2 - \sigma_3 = \sigma. \tag{25}$$

Analogous relations hold for the $N+1$ expansion. For internal consistency, in the calculation of $|GS\rangle$ one should include zero- and two-configuration states in the configuration interaction expansion. It was demonstrated elsewhere[54] that this procedure does not lead to a renormalization of the ground state: therefore, $|GS_{3BS}\rangle = |GS_0\rangle$. We are able to write the interacting GF as the matrix element of the propagator operator on the $|s^p\rangle$ states:

$$G^p_{ss'}(\omega) = \langle s^p|\frac{1}{z^p - H}|s'^p\rangle \tag{26}$$

where $|s'^p\rangle$ and $|s^p\rangle$ differ only in the band index and with $p=+,-$ for the electron and hole case according to the above definitions. We also note that, because the Hubbard Hamiltonian commutes with the total z component of the spin, $|GS\rangle$ can be chosen as an eigenstate of S_z, so that the GF is diagonal in the spin index σ (besides being diagonal in the $\mathbf{k}$ vector index by virtue of lattice symmetry).

By projecting the Hamiltonian on the $N-1$ electron states through the closure relation (the label "$-$" is dropped) $\Sigma_s|s\rangle\langle s| + \Sigma_t|t\rangle\langle t| = \mathbb{I}$, we obtain three terms:

$$H_1 = \sum_{ss'} |s\rangle\langle s|H|s'\rangle\langle s'|, \tag{27}$$

$$H_3 = \sum_{tt'} |t\rangle\langle t|H|t'\rangle\langle t'|, \tag{28}$$

$$V = \sum_{st} |s\rangle\langle s|H|t\rangle\langle t| + \text{h.c.}, \tag{29}$$

which give the Hamiltonian as $H \simeq H_1 + H_3 + V$. Defining the resolvent of the three-body interaction H_3 as

$$F_3(z) = \frac{1}{z - H_3}, \tag{30}$$

and following Ref. 54 we are able to write the GF as

$$G^-_{ss'}(\omega) = \left(z - H_1 ss' + \sum_{tt'} V_{st} F_{3tt'} V_{t's'}\right)^{-1}. \tag{31}$$

The last term on the rhs of Eq. (31) is an effective self-energy for the hole propagator only: we denote it Σ^-. Analogous relations are valid for the $N+1$ electron case. A detailed discussion of the theoretical framework of the methods (including the calculation of the three-body resolvent F_3) can be found in Ref. 54 and references therein.

The calculation of the resolvent operator and then of the SE's $\Sigma^\pm$ requires in input the projected density of states (pDOS's) related to the localized orbitals in the expression for the Hubbard Hamiltonian and directly extracted from the DFT calculation. The final expression for the hole and electron SE's according to the three-body formalism are then given as

$$\Sigma^\pm_{q\sigma}(\omega) = |q\sigma\rangle\Sigma^{\text{orb}\pm}_{q\sigma}(\omega)\langle q\sigma|, \tag{32}$$

where q's are the localized orbitals where Hubbard terms U and J are switched on. The terms $\Sigma^{\text{orb}\pm}_{q\sigma}(\omega)$ are the so-called *orbital self-energies* which are the output of the three-body scattering calculation. Once the SE is written by means of the atomic projectors as in Eq. (32) we can move back to the Bloch states by knowing the atomic projections of the band eigenvectors and then again to the WF basis by a further unitary transformation (which is known once the WF's have been calculated).

In order to obtain the time-ordered SE's (which are the needed objects to introduce correlation in the transport calculation) we must calculate both electron and hole GF's [from Eq. (31)]. As it is common in most approximated calculations, the correct analytic properties of the GF are not guaranteed and they can be recovered by considering only its imaginary part and determining anew the real part by Kramers-Krönig relations.[58] Another possibility, which is reliable and numerically stable when the occupations of the localized orbitals are far from half-filling,[54,59] is to do first the Kramers-Krönig transform on the imaginary part of the hole and electron orbital SE's, and then use the result as the full retarded self-energy. The latter is our choice in the remainder of this paper.

IV. RESULTS

Break-junction techniques[60] have recently obtained large success in producing ultimate nano-junctions. The realization of a break-junction is conceptually simple, although practically sophisticated: A metal wire is first etched and then mechanically stretched until it is broken. Due to the high mechanical precision of the procedure, tiny junctions and ultimate atomic contacts have been attained.[60] Some metals, such as gold, platinum, and iridium, are able to form[61–64] one-dimensional (1D) atomic chains of variable length. This fact has been recently[60] related to an interplay between localization of d orbitals and spin-orbit effects, which is typical of $5d$ transition metals. According to the above description, the system in a break-junction configuration is divided into two physically distinct regions: the massive bulk tips and the 1D wire in between them, as depicted in Fig. 1(a). From the point of view of short range electronic correlations it is expected that the 1D chain gives rise to larger effects than the bulk tips, because of a more prominent U/t ratio: we remind the reader that t is a measure of the average hopping terms of Eq. (21), hence of the band width. The increase of the U/t value in 1D systems is due to two simultaneous effects: (*i*) t decreases because of the band-width shrinking related to dimensionality effects, and (*ii*) the U parameter is expected to be larger in 1D than in 3D systems because of the less effective screening by the metallic environment.

Focusing on the case of late $5d$ transition metals, no important short-range correlation effects are expected in the

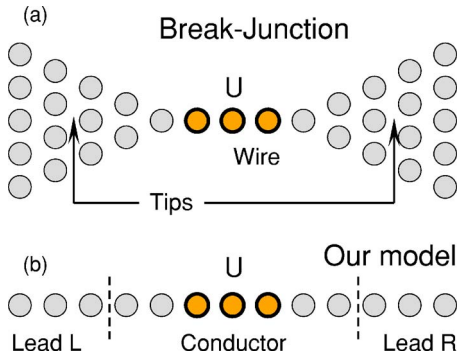

FIG. 1. (Color online) (a) Schematic geometry of a break-junction forming an atomic wire. (b) The atomic model that we adopt to highlight correlation effects. Circles represent platinum atoms: thin (thick) circles indicate atoms where the Hubbard term is $U=0$ (non-negligible, $U=2$ eV).

case of gold because of its closed d shell, whereas platinum and iridium may give rise to such effects. To confirm this intuitive vision and verify that a Pt break-junction is suitable to test our method, we perform an in-depth analysis of the Pt electronic structure, comparing the mean-field and the correlated spectral functions for the Pt 3D bulk and 1D wire. We adopt a Pt-Pt distance of 3 Å for the wire and a fcc cell of side $a=3.92$ Å for the bulk. The maximum kinetic energy for plane waves included in the basis set is 50 Ry and norm-conserving LDA pseudopotentials are used. In order to separate lateral replicas of the wire, we fix the supercell size to 10.6×10.6 Å^2 in the plane orthogonal to the atomic chain. The value $U=2.0$ eV is used for the Hubbard parameter when electronic correlation is switched on: this is a rough but conservative estimation, plausible for the bulk but quite low for the wire. Figure 2 reports the results of this comparison. It shows that bulk properties [Fig. 2(a)] are unchanged by the insertion of correlation terms in the electronic structure, whereas significant effects are noted for the wire [Fig. 2(b)], even in the conservative approximation chosen for U. In fact, in the 1D case we can observe a shift of the main d peak near the Fermi level E_F and the appearance of low-energy satellite structures (around −4.0 eV). This preliminary analysis confirms that correlation effects may play an important role in the Pt wire between two break-junction tips, due to dimensionality, whereas the effect on the tips themselves can be neglected due to the higher screening of the metallic bulk. This outcome fixes the framework for our choice for the model of a break-junction, explained in the following and shown in Fig. 1(b).

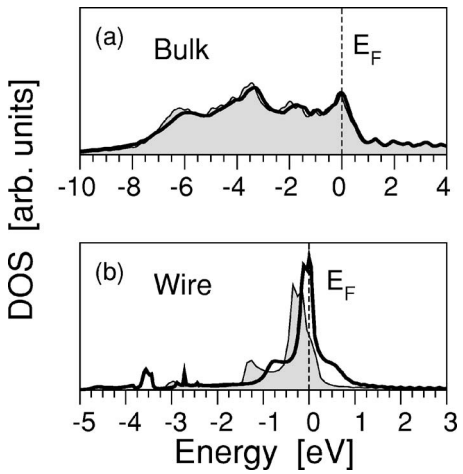

FIG. 2. Spectral functions for platinum: (a) periodic 3D fcc bulk system and (b) infinite 1D wire. Shaded areas are the mean-field DFT results, thick solid lines include many-body effects within the 3BS framework. The Fermi energy is set to zero in both panels. Spectral function scales are different in (a) and (b) and use arbitrary units.

In order to further investigate the inclusion of correlation effects on 1D atomic chains we focus our attention on a simplified junction model: we neglect the full complexity of the tip-wire interfaces and substitute the massive leads by semi-infinite mean-field platinum wires while the central conducting wire is treated at the many-body level. The substitution of the bulk leads with linear atomic chains is operated to make the prototype application of our method as simple as possible. The neglect of electronic correlations in the 1D leads is justified by the comparison just discussed above, in the sense that they should simulate 3D metals in which correlations are demonstrated to be ineffective [Fig. 2(a)]. The result of this modeling is an infinite wire having Hubbard U operative only on a finite number of Pt atoms, as illustrated in Fig. 1(b). Whereas this approximation misses an important contribution in the description of the true break-junction, it permits us to directly focus on the effect we want to analyze (e-e correlation), just leaving apart the widely studied and well-known effects of the contact resistance.[60,65] A comparative analysis including the effects of the contact interface is reported elsewhere.[29]

As described in Fig. 1(b), we divided our model system in the usual leads and conductor regions. We set up a conductor supercell containing 11 Pt atoms in order to have room for making the electron-electron interaction well decaying inside the cell, recovering the electronic structure of the leads at the interface. We checked that within these conditions we can correlate up to seven central atoms in the C cell (convergence details in the following). The lateral dimensions of the cell, the kinetic energy cutoff of plane waves, and the value of the Hubbard U parameter ($U=2.0$ eV) were chosen as before. We included four **k** points in the Brillouin zone summations in the DFT self-consistent calculation.

A. Electronic structure

We start with an in-depth discussion of the electronic structure for the Pt wire, to highlight the role of electronic correlation: The total and atom-projected DOS (pDOS) are reported in Fig. 3. Due to the cylindrical symmetry of the system with respect to the axis defined by the wire itself, the Hamiltonian commutes with the z component m of the total angular momentum, making m a good quantum number. It is therefore possible to distinguish among the atomic pDOS components according to m. In particular we identify the term corresponding to platinum d orbitals having $m=0$ as d_0 and those with $|m|=1$ ($|m|=2$) as $d_1(d_2)$ ($\pm m$ terms are de-

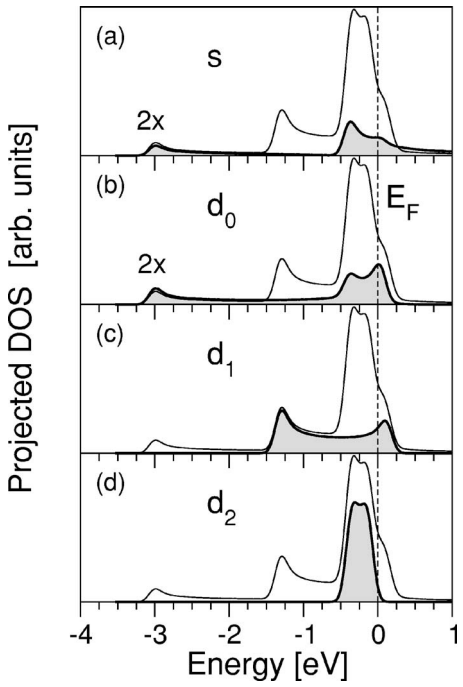

FIG. 3. Total and projected DOS for the mean-field Pt chain. In each panel, shaded areas represent the pDOS while thin lines are the reference total DOS. Vertical scales are the same for each graph. Panel (a) shows the Pt *s*-pDOS; (b), (c) and (d) the *d*-pDOS corresponding to $m=0$, $|m|=1$ and $|m|=2$, respectively. The Fermi energy is set to zero. pDOS in panels (a) and (b) have been magnified by a factor of 2 for clearness.

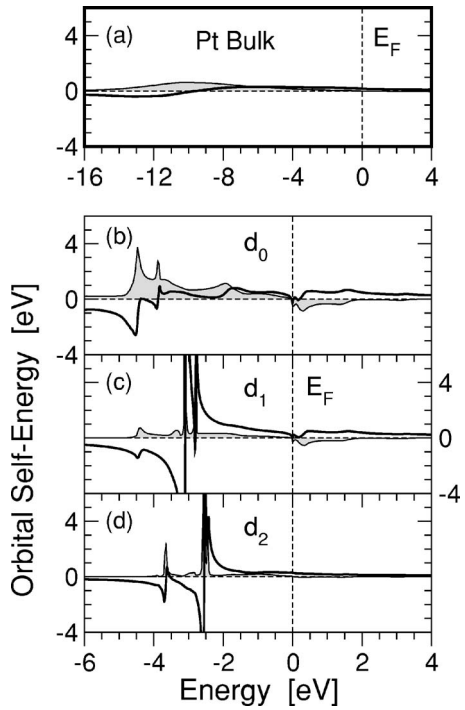

FIG. 4. Orbital self-energies. (a) The largest orbital SE of Pt fcc bulk (reported as reference). Inequivalent orbital SE's for (b) d_0, (c) d_1, and (d) d_2. The energy scale of panel (a) is different but the SE scale is maintained equal to the others. Solid lines (shaded areas) give the real (imaginary) part of the self-energies. The Fermi energy is set to zero. The wells in the real and imaginary SE's near the Fermi level are probably connected to the numerical matching of hole and electron GF's (see Sec. III B).

generate). Figure 3 shows that, as expected on the basis of symmetry constraints, *s* and d_0 states are strongly hybridized (same peaks and band widths in the pDOS) while d_1 and d_2 remain pure narrow-band *d* states (in a simple *s*-*d* picture). The *s* and d_0 states can mix because they have the same *m* quantum number. In Table I we report a summary of some parameters (including band widths and occupations) that describe the electronic structure of the system. We find an effective number of 1.06 *d* holes per atom. The importance of correlation effects is related both to the strength of the *e*-*e* interaction U/t and to the band occupation. In the extreme case of a completely filled band, where in the 3BS picture no *e*-*h* pairs can be added, correlation effects are absent, irrespectively of the strength of the *e*-*e* interaction. In this case, even a tiny number of holes is sufficient to activate correlation effects. The present case with $U/t \simeq 1$ and one hole out of ten *d* states can be defined as a regime of relatively high correlation.

TABLE I. Atomic projected DOS (*sd* states) description. Occupations account for spin and are referred to singly degenerate orbitals.

	s	d_0	d_1	d_2
Degeneracy	1	1	2	2
Band width (eV)	~10	3.60	1.90	0.75
Occupation	1.05	1.68	1.67	1.98
Hole no.	0.95	0.32	0.33	0.04

Starting from the projection of Bloch states onto atomic orbitals we apply the 3BS formalism to compute the many-body corrections. As described in Eq. (32), the self-energy operator in the 3BS scheme is written as a sum of projectors onto localized states. This particular form of the SE defines the so-called orbital SE's that are reported in Fig. 4. Since the SE operator is non-Hermitian by definition, the orbital SE's are complex functions: the real part tends to shift the position of the quasi-particle (QP) poles, while the imaginary part accounts for finite QP lifetimes. In a simplified picture (neglecting the sd_0 Hamiltonian coupling term), the inversion of the Dyson equation would lead to poles for the interacting GF given by the solutions of the equation $\omega - \epsilon_{d_m} = \Sigma^{\mathrm{orb}}_{d_m}(\omega)$, where the ω energy is defined on the entire complex plane and ϵ_{d_m} runs over all the eigenvalues corresponding to d_m symmetry. If ω is constrained on the real axis, the spectral function would exhibit a strong peak where $\omega - \epsilon_{d_m}$ intercepts the real part of the orbital self-energy $\Sigma^{\mathrm{orb}}_{d_m}(\omega)$. The imaginary part of the SE would fix the energy width of such a peak.[58]

Using this kind of analysis we can compare the different *d* components of the wire orbital SE's [Figs. 4(b)–4(d)]. Figure 4(a) shows as a reference the largest orbital SE obtained for Pt bulk: it is spread over a broad energy range and the intensity is much smaller than the orbital self-energies of the wire. Indeed, the main difference among wire and bulk is in the

order of magnitude of the orbital SE's: this is due to the fact that wire and bulk are characterized by very different U/t ratios. The energy range where correlation effects are important is also quite different in the two cases: while the bulk orbital SE of Fig. 4(a) is non-negligible at energies lower than 6–8 eV, the wire orbital SE's of Figs. 4(b)–4(d) are dominant in an energy range much closer to Fermi energy. This property can be inferred also from Fig. 2: the only slight correction in the bulk spectral function [Fig. 2(a)] occurs in the low-energy region, whereas the wire undergoes corrections well around Fermi energy [Fig. 2(b)]. In Figs. 4(b)–4(d) we analyze the details of SE's with different angular momenta. All the peaks in the d_0 SE occur at energy values where the d_0-pDOS is nonvanishing [Fig. 3(b)]. Therefore, they effectively modify the electronic structure and contribute to the appearance of satellite peaks in the total DOS of the wire. In particular, the low-energy peaks of the d_0-SE account for the satellite structures around −4.0 eV in the DOS of Fig. 2(b). At higher energies, the d_0-SE peaks are responsible both for the satellite structures and for the short-lifetime states closer to the Fermi level, which are expected to play a major role in transport phenomena. Conversely, the spike-like peaks in the d_1 and d_2 SE's are unable to produce any spectral features, because they occur at energy values where the corresponding pDOS curves are zero.

To close this section, let us remark on a few technical aspects that allow for efficient simulations with our simple atomic model in which we want only selected atoms to carry many-body effects. Because of the particular form of the 3BS self-energy, we can easily switch on the correlation on a variable set of platinum atoms in the linear chain, just by including the d orbitals of the chosen atoms in the sum over projectors in Eq. (32). Therefore, the analysis of the orbital SE's applies both to the case of the infinite correlated wire illustrated above and to the atomic model of Fig. 1(b). We further note that the Wannier functions do not change with the number of correlated atoms, because they depend exclusively on the mean-field electronic structure. Therefore, they are computed only once for the Pt wire and used for different numbers of correlated atoms. Six WF's for each atom describe the sd states. In the MLWF basis set for the Pt wire computed as described in Sec. III A, we found four WF's which are quite similar to the atomic states with $|m|=1,2$, and 2 WF's which differ significantly from the atomic orbitals. This result reflects the strong s-d_0 hybridization discussed earlier. Numerically, the 3BS self-energy operator on the MLWF basis set is found to decay on the nearest neighbor atoms of the many-body region, validating the assumptions on the SE localization previously described.

B. Transport properties

In this section we focus on the transport properties of the prototype platinum chain. The curves computed for the effective transmittance as a function of energy are reported in Fig. 5, for various numbers N of correlated atoms in the wire. The step-like noninteracting transmittance is given as a reference (thin line in both the main plot and inset). The case of $N=3$ correlated atoms is shown in the main panel and discussed in more detail in the text. The most evident feature that stems from the inclusion of the electron-electron interaction is a strong quenching of the transmittance in the hole region of the spectrum, while no important modifications occur above the Fermi level. The physical reason can be found in the shapes of the SE's, which are almost completely confined below the Fermi energy (see Fig. 4), a consequence of the large occupation of d-electrons in platinum (Table I).

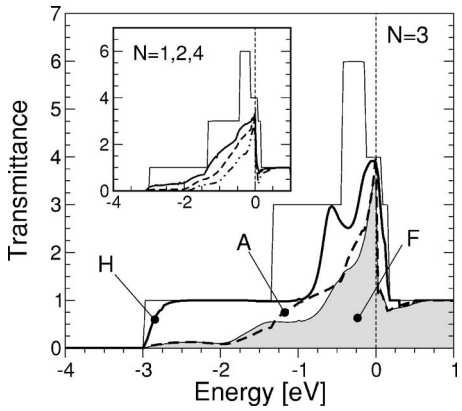

FIG. 5. Effective transmittance of the Pt atomic chain for different numbers of correlated atoms N, i.e., atoms in which the many-body e-e interaction operates. Main plot: Calculated effective transmittances for $N=3$ correlated atoms, obtained using the Hermitian part of the SE (H, solid thick line), the anti-Hermitian part (A, dashed line), or the full physical SE (F, shaded area). Inset: transmittances (obtained using the full SE's) for $N=1$ (solid line), 2 (dashed line), and 4 (dot-dashed line) correlated atoms.

Moving from one to four correlated atoms we can observe an even larger depletion of the hole transmittance. This finding supports the idea that electron-electron interactions in a platinum wire tend to freeze the holes, making transport to occur via electron carriers.

As was mentioned before, the very nature of the electron correlation is enforced by a SE operator which is dynamical (energy dependent) and non-Hermitian. We pointed out in a previous work[29] that proper and important effects of introducing correlation on the effective transmittance are linked to the presence of an anti-Hermitian (imaginary) component of the SE. In order to support the latter statement, we studied the transmittance separately for each angular momentum channel (d_0+s, d_1, d_2), also dividing the effect of their Hermitian (H) and anti-Hermitian (A) parts. This last operation can be rigorously defined because the SE can be written as a sum of H and A parts, $\Sigma(\omega)=\Sigma^H(\omega)+\Sigma^A(\omega)$, where

$$\Sigma^H(\omega) = \tfrac{1}{2}[\Sigma(\omega) + \Sigma^\dagger(\omega)], \tag{33}$$

$$\Sigma^A(\omega) = \tfrac{1}{2}[\Sigma(\omega) - \Sigma^\dagger(\omega)]. \tag{34}$$

The transmittances obtained in this way for the case of an $N=3$ correlated atom wire are reported in Fig. 6 (see the caption for a full explanation of the curves). Focusing on Fig. 6(a), which describes the transmittance for the d_0+s component, we note that the result of the complex SE (shaded area) is almost superimposed to that due to the anti-

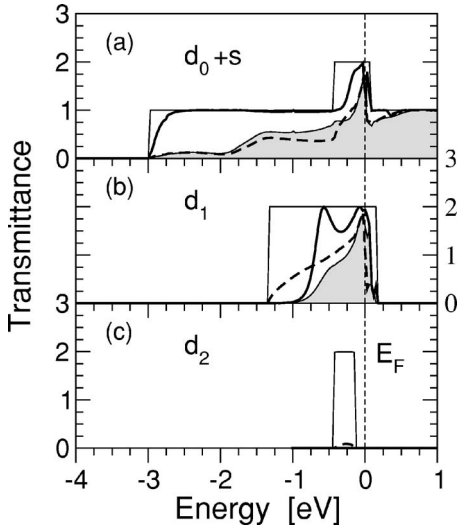

FIG. 6. Effective transmittance resolved for different angular momentum channels in the case of three correlated atoms in the Pt wire. Panels (a), (b), and (c) report the results for the d_0+s, d_1, and d_2 components. In each panel solid (dashed) thick lines describe the results obtained with the $H(A)$ part of the SE, the shaded area is the transmittance obtained by using the complex SE (both Hermitian and anti-Hermitian components), and the thin solid line is the reference mean-field transmittance for each channel.

Hermitian SE (dashed thick line), while the one related to the Hermitian SE (solid thick line) is very similar to the mean-field case, except for the smoothing below −2.5 eV and for the narrow peak near −0.5 eV. Figure 6(b) describes the effective transmittance for the d_1 channel. In contrast with the d_0+s case, we see that both the H and A parts of the d_1 SE have a non-negligible role in the computed effective transmittance. In the case of d_2, reported in Fig. 6(c), both A and H components of the SE are responsible for quenching the mean-field peak. As expected, the transmittance is mainly given by the d_0+s component, which is the least localized and most itinerant of all the analyzed components (as inferred from the high band-width values).

We can easily read the above results in terms of a simple *sd* model. Due to the symmetry of the problem, only the s and the d_0 terms can be coupled by the *e-e* Hamiltonian, whereas d_1 and d_2 states maintain a pure d character. This makes the d_0 band largely more dispersive than the other d-like terms. From the point of view of correlation, the orbital SE's (which take components from every d state) are mainly due to the localized states d_1 and d_2 which have larger U/t ratios. The transmittance of these channels is strongly suppressed. On the other hand the d_0 SE becomes itself more effective due to the localization of d_1 and d_2 and corrects DOS and transmittance on the whole hole energy range. The emerged scenario is thus based on a sort of interplay between localization and itinerancy: the former introduces correlation effects, the latter links correlation to transport.

The ultimate effect of the SE on the effective transmittance is the sum of the various angular momentum channels d_0+s, d_1, d_2, and is shown in Fig. 5, divided into H and A contributions (solid and dashed lines, respectively). The anti-Hermitian part of the self-energy (dashed line in Fig. 5) gives a transmittance which is very close to the one obtained using the whole complex SE, which bears the physical meaning. This outcome is very significative: It stresses the key role of the finite lifetimes of quasi-particles in the case of transport in correlated systems. In fact, the real part of the SE is responsible for energy shifts of the peaks in the DOS (hence, in the transmittance), whereas the imaginary part is responsible for spreading of the peaks, indicative of finite lifetimes. Let us additionally point out that the presence of an interface between the conductor and the leads (which is neglected here) is expected to lower the importance of the real part of the SE, further enhancing the effects of the imaginary part. This follows because the H self-energy in the present case contributes to misalign levels between conductor and leads, while the introduction of massive leads means increasing the spectrum of available states for conduction, thereby making misalignment less effective.

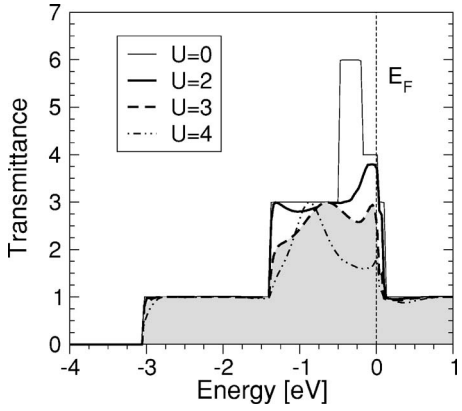

FIG. 7. Transmittance versus energy calculated by means of LDA+U for various values of the Hubbard parameter U.

C. 3BS versus LDA+U

In order to further analyze the very effect of the electron-electron scattering carried by the non-Hermiticity of the correlation SE, we performed some LDA+U[34–36] calculations of the electronic and transport properties of the Pt wire. LDA+U is the standard method for adding short-range correlation contributions to the mean-field DFT electronic structure. This approach corrects the total energy with a specific Hubbard term, which is introduced in the Kohn and Sham Hamiltonian as a non-local mean-field potential, Hermitian by definition. Therefore, the method can describe energy shifts due to many-body coupling, but is not able to treat quasi-particle lifetimes. We compare the LDA+U (Fig. 7) with the 3BS results (Fig. 5): the latter incorporate the full dynamic and non-Hermitian SE. The LDA+U calculations were performed in the same geometry of Fig. 1(b) and using the same parameters for **k**-point sampling and cell dimensions. Nonzero Hubbard U values were taken into account only on the three central atoms in the conductor, thus comparing to the $N=3$ case of Fig. 5. The calculation of U was not performed self-consistently,[66] but several values were tested. Since it is not easy to compare U integrals used in

calculations with different methods (3BS and LDA+U) we analyze U values in a viable range.

In Fig. 7 we report the transmittance curves obtained for $U=2,3,4$ eV. We observe that the $U=4$ curve presents a large well close to the Fermi energy, suggesting that for this value one gets close to the Mott-Hubbard metal-insulator transition. This value is therefore to be considered already out of the regime that we studied in this paper. We also checked the case with $U=6$ eV and indeed found a scenario very close to the insulating behavior. From the analysis of the curves reported in Fig. 7 we suggest that the value of $U=2.0$ eV that we used within the 3BS method is comparable to the range $U=2-3$ eV in the LDA+U scheme: we take the $U=3$ curve (shaded area, dashed line) in Fig. 7 as the reference calculation. Comparing the two sets of results (shaded areas in Figs. 5 and 7) we see that only the main features due to the Hermitian part of the SE are reproduced in the LDA+U calculation. In particular, the two peaks around -1.0 eV and the Fermi energy in Fig. 7 correspond to those near -0.8 eV and the Fermi energy in Fig. 5. A direct comparison is not straightforward because the exact equivalent values of U in the two approaches are not known and can only be estimated. However, the observation that the static Hermitian LDA+U potential reproduces only the effects given by the dynamic Hermitian part of the 3BS SE underline the larger extent of our method in the description of correlated transport phenomena. While the dynamical nature of the SE is fundamental for studying the low level satellite structures found in the photoemission experiments, here the main role is played by the anti-Hermitian component of the SE in a sufficiently large neighborhood of the Fermi energy.

V. CONCLUSIONS

In this paper we presented a formalism for electronic transport through spatial regions hosting interacting charge carriers, suitable for *ab initio* implementations. As a first step of our formalism, we recast a well-known expression for the current[37] in a Landauer-like form using an *ansatz* to relate greater and lesser Green's functions to advanced and retarded Green's functions.[43] From the Landauer-like formula for the current in a correlated conductor, we then defined an *effective* transmittance. The computation of the latter quantity may unravel the effects of electronic correlation on transport. We numerically implemented the method in the WANT package,[33] which describes transport by means of the matrix Green's function technique using maximally localized Wannier functions as real space basis set. Many-body terms in the electronic structure were included following the nonperturbative three body scattering formalism.[53,54] We focused our analysis on the case of short-range electron-electron interactions (Anderson regime) and applied the formalism to an atomic platinum chain, where only some atoms are considered beyond the mean-field regime, as a schematic simulator of break-junction experiments.

Our results indicate that short-range many-body interactions influence the transport properties. The specific nature of the correlation gives rise to quasi-particle spectral features which include the renormalization of energy levels and the appearance of finite lifetimes. The latter are found to be the dominant feature in determining the shape of the effective conductance of the correlated conductor. Indeed, a direct comparison with LDA+U results for the same system shows that the inclusion of finite lifetimes, neglected in the LDA+U approach and accounted for in the 3BS method, is needed to describe the major effects of transmittance quenching.

ACKNOWLEDGMENTS

We acknowledge M. Buongiorno Nardelli, M. J. Caldas, E. Molinari, C. Jacoboni, C. Calandra, and G. Bussi for supporting this work with stimulating and fruitful discussions. Funding was provided by the EC through Project No. IST-2001-38951 and TMR network "Exciting," by INFM through "Commissione Calcolo Parallelo," and by MIUR (Italy) through "FIRB-NOMADE."

APPENDIX: KELDYSH FORMALISM IN DEVICE CONFIGURATION

For the sake of completeness, we report a derivation of the final form of Eqs. (7) and (8) presented in this paper, starting from the general nonequilibrium Green's functions (NEGF's) formalism as proposed by Keldysh. This is particularly useful in view of the study of interacting conductors. More detailed descriptions can be found in Refs. 38–40 and references therein. It is important to remark that in the original Keldysh formalism no distinction is made between different parts of the investigated system, whereas in our approach the target system is a *L-C-R* junction, where it is important to describe the relevant quantities (GF's and SE's) as block matrices in the L,C,R zones. Hence, this appendix is essentially devoted to establishing a connection between the SE operators spread over the whole many-body system (denoted with a $\tilde{}$ overhead in this appendix) and the same operators in a block-matrix form in the conductor region (denoted with a C subscript).

The starting point is fixed by the coupled equations involving the retarded, advanced, and lesser GF's for the whole system, that is, in the cases of interest for us, the sum of the L,C,R regions:

$$G^r = G_0^r + G_0^r \tilde{\Sigma}^r G^r, \tag{A1}$$

$$G^< = (\mathbb{I} + G^r \tilde{\Sigma}^r) G_0^< (\mathbb{I} + \tilde{\Sigma}^a G^a) + G^r \tilde{\Sigma}^< G^a. \tag{A2}$$

The G_0 GF's are related to a noninteracting out-of-equilibrium reference state and the self-energies (SE's) account for the inclusion of the interactions. In our target *L-C-R* problem all the GF's and SE's can be cast in a 3×3 block-matrix form defined on the L,C,R regions. The purpose of this appendix is to show a procedure by which Eqs. (A1) and (A2) can be modified in order to extract some expressions for the conductor-diagonal block of the GF's.

The Dyson equation [Eq. (A1)] can be rewritten in the final form of Eq. (8) by introducing the lead self-energies defined as

$$\Sigma_X^{r,a} = (H_{CX} + \tilde{\Sigma}_{CX}^r) g_X^{r,a} (H_{XC} + \tilde{\Sigma}_{XC}^r), \quad X = L,R, \quad \text{(A3)}$$

and adding them to the C block $\tilde{\Sigma}_C^r$ of $\tilde{\Sigma}^r$. This comes from a direct inversion of the 3×3 block matrix $\omega\mathbb{I} - H - \Sigma^r$. Note that the above definition of the lead SE's differs from the one given in Eq. (6) because of the presence of the nondiagonal $\tilde{\Sigma}_{CX}^r$ block elements. When the SE decays inside the C region (eventually making the conductor larger and larger), $\tilde{\Sigma}_{CX}^r$ can be neglected, thus justifying Eq. (6). In systems where this approximation does not hold, the expressions in Eq. (6) should be updated as in Eq. (A3). The final effective self-energy thus reads

$$\Sigma_C^r = \Sigma_L^r + \Sigma_R^r + \tilde{\Sigma}_C^r, \quad \text{(A4)}$$

which is the one given in Eq. (13), once we set $\Sigma_{corr}^r = \tilde{\Sigma}_C^r$. The sum in Eq. (A4) defines the conductor self-energy of Eq. (8).

To obtain instead Eq. (7) from the general Keldysh formalism, we observe that it is possible to write the *equilibrium mean-field* lesser GF as

$$G_{0,eq}^< = G_{0,eq}^r \tilde{\Sigma}_{0,eq}^< G_{0,eq}^a, \quad \text{(A5)}$$

where $\tilde{\Sigma}_{0,eq}^< = 2 f_{eq}(\omega)\eta^+ \mathbb{I}$ and η^+ is the limit $\eta \to 0^+$. Therefore, using the same Eq. (7), with the initial state the *equilibrium mean-field* system and the final state the *nonequilibrium mean-field* system, one obtains

$$G_{0,neq}^< = G_{0,neq}^r (\tilde{\Sigma}_{0,eq}^< + \tilde{\Sigma}_{0,neq}^<) G_{0,neq}^a, \quad \text{(A6)}$$

where $\tilde{\Sigma}_{0,neq}^<$ accounts for the nonequilibrium properties of $G_{0,neq}^<$. In the same way, it is possible to add the full *nonequilibrium many-body* correction by adding a suitable SE operator $\tilde{\Sigma}^<$:

$$G^< = G^r (\tilde{\Sigma}_{0,eq}^< + \tilde{\Sigma}_{0,neq}^< + \tilde{\Sigma}^<) G^a. \quad \text{(A7)}$$

This last expression describes the lesser GF we are interested in for transport calculations.

We make explicit use of the assumption that the $\tilde{\Sigma}_{0,neq}^<$ and $\tilde{\Sigma}^<$ SE's can be neglected out of the conductor-diagonal block, or described as constant mean-field terms in the L or R diagonal blocks. This accounts for a possible rigid shift of energy levels. The operation is viable by virtue of the fact that the system is out-of-equilibrium and interacting only in the conductor region. Within the above discussed approximations the expression for the C block of the lesser GF reads

$$\begin{aligned} G_C^<(\omega) = {} & G_{CL}^r (\tilde{\Sigma}_{0,eqL}^< + \tilde{\Sigma}_{0,neqL}^<) G_{LC}^a \\ & + G_C^r (\tilde{\Sigma}_{0,eqC}^< + \tilde{\Sigma}_{0,neqC}^< + \tilde{\Sigma}_C^<) G_C^a \\ & + G_{CR}^r (\tilde{\Sigma}_{0,eqR}^< + \tilde{\Sigma}_{0,neqR}^<) G_{RC}^a. \end{aligned} \quad \text{(A8)}$$

Using the same techniques as for the retarded, advanced lead SE's it is possible to derive

$$\begin{aligned} G_{LC}^{r,a} &= g_L^{r,a} H_{LC} G_C^{r,a}, \\ G_{RC}^{r,a} &= g_R^{r,a} H_{RC} G_C^{r,a}, \\ G_{CL}^{r,a} &= G_C^{r,a} H_{CL} g_L^{r,a}, \\ G_{CR}^{r,a} &= G_C^{r,a} H_{CR} g_R^{r,a}, \end{aligned} \quad \text{(A9)}$$

which finally give

$$G_C^<(\omega) = G_C^r (\Sigma_L^< + \Sigma_R^< + \tilde{\Sigma}_{0,eqC}^< + \tilde{\Sigma}_{0,neqC}^< + \tilde{\Sigma}_C^<) G_C^a. \quad \text{(A10)}$$

Here the definitions of the lead lesser SE's are coherent with the ones given in Eq. (6).

It should be noted that, whereas some other SE's persist, the $\tilde{\Sigma}_{0,eqC}^<$ and $\tilde{\Sigma}_{0,neqC}^<$ terms in Eq. (A10) can be neglected because the η^+ term is overcome by other leading terms. These approximations lead to the final expression for the lesser self-energy as $\Sigma_C^< = \Sigma_L^< + \Sigma_R^< + \Sigma_{corr}^<$, where $\Sigma_{corr}^< = \tilde{\Sigma}_C^<$, as given in Sec. II B after Eq. (13).

*Corresponding author. E-mail address: ferretti.andrea@unimore.it

[1] M. A. Reed, C. Zhou, C. J. Muller, T. P. Burgin, and J. M. Tour, Science **278**, 252 (1997).
[2] Z. Yao, H. W. C. Postma, L. Balents, and C. Dekker, Nature (London) **402**, 273 (1999).
[3] C. Joachim, J. K. Gimzewski, and A. Aviram, Nature (London) **408**, 541 (2000).
[4] J. M. Tour, Acc. Chem. Res. **33**, 791 (2000).
[5] J. M. Seminario, A. G. Zacarias, and P. A. Derosa, J. Phys. Chem. A **5**, 791 (2001).
[6] J. G. Park, G. T. Kim, J. H. Park, H. Y. Yu, G. McIntosh, V. Krstic, S. H. Jhang, B. Kim, S. H. Lee, S. W. Lee, M. Burghard, S. Roth, and Y. W. Park, Thin Solid Films **393**, 161 (2001).
[7] J. Reichert, R. Ochs, D. Beckmann, H. B. Weber, M. Mayor, and H. v. Löhneysen, Phys. Rev. Lett. **88**, 176804 (2002).
[8] C. Loppacher, M. Guggisberg, O. Pfeiffer, E. Meyer, M. Bammerlin, R. Luthi, R. Schlittler, J. K. Gimzewski, H. Tang, and C. Joachim, Phys. Rev. Lett. **90**, 066107 (2003).
[9] R. M. Metzger, Chem. Rev. (Washington, D.C.) **103**, 3803 (2003).
[10] G.-H. Kim and T.-S. Kim, Phys. Rev. Lett. **92**, 137203 (2004).
[11] S. Li, Z. Yu, S.-F. Yen, W. C. Tang, and P. J. Burke, Nano Lett. **4**, 753 (2004).
[12] J. Taylor, H. Guo, and J. Wang, Phys. Rev. B **63**, 245407 (2001).
[13] Y. Xue, S. Datta, and M. A. Ratner, Chem. Phys. **281**, 151 (2002).
[14] M. Brandbyge, J.-L. Mozos, P. Ordejón, J. Taylor, and K. Stokbro, Phys. Rev. B **65**, 165401 (2002).
[15] F. Evers, F. Weigend, and M. Koentopp, Phys. Rev. B **69**, 235411 (2004).

[16] D. Ferry and S. M. Goodnik, *Transport in Nanosctructures* (Cambridge University Press, Cambridge, 1997).
[17] S. J. Tans, M. H. Devoret, R. J. A. Groeneveld, and C. Dekker, Nature (London) **394**, 761 (1998).
[18] W. A. Schoonveld, J. Wildeman, D. Fichou, P. A. Bobbert, B. J. van Wees, and T. M. Klapwijk, Nature (London) **404**, 977 (2000).
[19] J. Park, A. N. Pasupathy, J. I. Goldsmith, C. Chang, Y. Yaish, J. R. P. M. Rinkoski, J. P. Sethna, H. D. Abrunña, P. L. McEuen, and D. C. Ralph, Nature (London) **417**, 722 (2002).
[20] P. Jarillo-Herrero, S. Sapmaz, C. Dekker, L. P. Kouwenhoven, and H. S. J. van der Zant, Nature (London) **429**, 389 (2004).
[21] T. W. Odom, J.-L. Huang, C. L. Cheung, and C. M. Lieber, Science **290**, 1549 (2000).
[22] W. Liang, M. P. Shores, M. Bockrath, J. R. Long, and H. Park, Nature (London) **417**, 725 (2002).
[23] M. Bockrath, D. H. Cobden, J. Lu, A. G. Rinzler, R. E. Smalley, L. Balents, and P. L. McEuen, Nature (London) **397**, 598 (1999).
[24] J. N. Crain, A. Kirakosian, K. N. Altmann, C. Bromberger, S. C. Erwin, J. L. McChesney, J.-L. Lin, and F. J. Himpsel, Phys. Rev. Lett. **90**, 176805 (2003).
[25] D. S. Kosov, J. Chem. Phys. **119**, 1 (2003).
[26] N. T. Maitra, I. Souza, and K. Burke, Phys. Rev. B **68**, 045109 (2003).
[27] P. Delaney and J. C. Greer, Phys. Rev. Lett. **93**, 036805 (2004).
[28] Y.-C. Chen, M. Zwolak, and M. Di Ventra, Nano Lett. **4**, 1709 (2004).
[29] A. Ferretti, A. Calzolari, R. Di Felice, F. Manghi, M. J. Caldas, M. B. Nardelli, and E. Molinari, Phys. Rev. Lett. **94**, 116802 (2005).
[30] N. Marzari and D. Vanderbilt, Phys. Rev. B **56**, 12847 (1997).
[31] I. Souza, N. Marzari, and D. Vanderbilt, Phys. Rev. B **65**, 035109 (2002).
[32] M. Buongiorno Nardelli, Phys. Rev. B **60**, 7828 (1999).
[33] We used the *WanT* code, publicly available at http://www.wannier-transport.org. For details, see also Ref. 55.
[34] V. I. Anisimov, J. Zaanen, and O. K. Andersen, Phys. Rev. B **44**, 943 (1991).
[35] A. I. Liechtenstein, V. I. Anisimov, and J. Zaanen, Phys. Rev. B **52**, R5467 (1995).
[36] V. I. Anisimov, F. Aryasetiawan, and A. I. Lichtenstein, J. Phys.: Condens. Matter **9**, 767 (1997).
[37] Y. Meir and N. S. Wingreen, Phys. Rev. Lett. **68**, 2512 (1992).
[38] H. Haug and A.-P. Jauho, *Quantum Kinetics in Transport and Optics of Semiconductors* (Springer, Berlin, 1996).
[39] J. Rammer and H. Smith, Rev. Mod. Phys. **58**, 323 (1986).
[40] A.-P. Jauho, N. S. Wingreen, and Y. Meir, Phys. Rev. B **50**, 5528 (1994).
[41] R. Landauer, Philos. Mag. **21**, 863 (1970).
[42] D. S. Fisher and P. A. Lee, Phys. Rev. B **23**, R6851 (1981).
[43] T.-K. Ng, Phys. Rev. Lett. **76**, 487 (1996).
[44] N. Sergueev, Q. F. Sun, H. Guo, B. G. Wang, and J. Wang, Phys. Rev. B **65**, 165303 (2002).
[45] P. Zhang, Q.-K. Xue, Y. P. Wang, and X. C. Xie, Phys. Rev. Lett. **89**, 286803 (2002).
[46] H.-F. Mu, G. Su, Q.-R. Zheng, and B. Jin, Phys. Rev. B **71**, 064412 (2005).
[47] G. Stefanucci and C.-O. Almbladh, Phys. Rev. B **69**, 195318 (2004).
[48] K. Burke, M. Koentopp, and F. Evers, cond-mat/0502385.
[49] E. Runge and E. K. U. Gross, Phys. Rev. Lett. **52**, 997 (1984).
[50] G. Vignale and W. Kohn, Phys. Rev. Lett. **77**, 2037 (1996).
[51] F. Bruneval, F. Sottile, V. Olevano, R. Del Sole, and L. Reining, Phys. Rev. Lett. **94**, 186402 (2005).
[52] G. D. Mahan, *Many-Particle Physics* (Plenum, New York, 1981).
[53] C. Calandra and F. Manghi, Phys. Rev. B **50**, 2061 (1994).
[54] F. Manghi, V. Bellini, and C. Arcangeli, Phys. Rev. B **56**, 7149 (1997).
[55] A. Calzolari, N. Marzari, I. Souza, and M. Buongiorno Nardelli, Phys. Rev. B **69**, 035108 (2004).
[56] S. Baroni, A. Dal Corso, S. de Gironcoli, and P. Giannozzi, 2001, http://www.pwscf.org.
[57] B. Farid, "Ground and low-lying excited states of interacting electron systems; a survey and some critical analyses," in *Electron Correlation in the Solid State*, edited by N. H. March (Imperial College Press, London, 1999), pp. 103–261.
[58] A. L. Fetter and J. D. Walecka, *Quantum Theory of Many-Particle Systems* (McGraw-Hill, New York, 1971).
[59] S. Monastra, F. Manghi, and C. Ambrosch-Draxl, Phys. Rev. B **64**, 020507(R) (2001).
[60] N. Agraït, A. L. Yeyati, and J. M. van Ruitenbeek, Phys. Rep. **377**, 81 (2003).
[61] H. Ohnishi, Y. Kondo, and K. Takayanagi, Nature (London) **395**, 780 (1998).
[62] A. Yanson, G. R. Bollinger, H. van den Brom, N. Agraït, and J. M. van Ruitenbeek, Nature (London) **395**, 783 (1998).
[63] V. Rodrigues, T. Fuhrer, and D. Ugarte, Phys. Rev. Lett. **85**, 4124 (2000).
[64] R. H. M. Smit, C. Untiedt, A. I. Yanson, and J. M. van Ruitenbeek, Phys. Rev. Lett. **87**, 266102 (2001).
[65] S. Datta, *Electronic Transport in Mesoscopic Systems* (Cambridge University Press, Cambridge, 1995).
[66] M. Cococcioni and S. de Gironcoli, Phys. Rev. B **71**, 035105 (2005).